

# Theoretical Prediction of Magnetic Exchange Coupling Constants from Broken-Symmetry Coupled Cluster Calculations

Henry F. Schurkus,<sup>1</sup> Dian-Teng Chen,<sup>2</sup> Hai-Ping Cheng,<sup>2</sup> Garnet Kin-Lic Chan,<sup>1</sup> and John F. Stanton<sup>3</sup>

<sup>1</sup>*Division of Chemistry and Chemical Engineering, California Institute of Technology, Pasadena, CA 91125*

<sup>2</sup>*Department of Physics, University of Florida, Gainesville, FL 32611*

<sup>3</sup>*Department of Chemistry, University of Florida, Gainesville, FL 32611*

Exchange coupling constants ( $J$ ) are fundamental to the understanding of spin spectra of magnetic systems. Here we investigate the broken-symmetry (BS) approaches of Noodleman and Yamaguchi in conjunction with coupled cluster (CC) methods to obtain exchange couplings.  $J$  values calculated from CC in this fashion converge smoothly towards the FCI result with increasing level of CC excitation. We compare this BS-CC scheme to the complementary EOM-CC approach on a selection of bridged molecular cases and give results from a few other methodologies for context.

## I. INTRODUCTION

The energy level structure of spin states is fundamental to the description of magnetism in molecules and materials. For molecules with localized spins on different atoms, the low-energy spin-states can often be qualitatively understood in terms of the phenomenological Heisenberg model<sup>1-3</sup>

$$H = -2 \sum_{A,B>A} J_{AB} \mathbf{S}_A \cdot \mathbf{S}_B \quad (1)$$

where  $A$  and  $B$  index the “spin centers”. The Heisenberg model is completely parametrized by the magnetic exchange coupling constant,  $J_{AB}$ , for each spin interaction  $A - B$ .

Estimating the exchange coupling, and its geometric dependence, is complicated by the fact that the underlying mechanism of spin-interactions is a multi-electron process, such as Anderson super-exchange;<sup>4</sup> furthermore, the low spin electron configurations that often appear in such investigations are a formidable challenge to quantum chemical methods. The most commonly-used approach involves calculations with density functional theory (DFT). Although DFT is ill-suited to describe eigenstates of the Heisenberg model, which possess multireference character arising from the largely independent spin orientations of the different centers, correctly parametrizing the model only requires us to match the energies of low-energy states, which need not be chosen as eigenstates. Consequently, it is commonly found that approaches based on broken-symmetry (BS) spin states such as the ones proposed by Noodleman<sup>5</sup> and Yamaguchi<sup>6</sup> can give estimates of  $J$  that are qualitatively comparable to experimentally-extracted values, even in cases where the exchange coupling arises due to super-exchange.<sup>7-14</sup> Still it is worthwhile to explore more sophisticated approaches within electronic structure, as this potentially permits the intrinsic Heisenberg energy level structure to be predicted with quantitative accuracy.

Coupled cluster (CC) theory is often used to generate benchmark quality descriptions of molecular proper-

ties.<sup>15</sup> Recently, Mayhall and Head-Gordon used spin-flip equation-of-motion (EOM) CC methods to obtain exchange couplings,<sup>16</sup> based on using CC and EOM-CC to approximate the two eigenstates of highest and next-highest spin described by the Heisenberg model. However, as mentioned, it is not necessary to target spin-eigenstates when parametrizing the Heisenberg model. Here we adopt the broken-symmetry methods of Noodleman and Yamaguchi in conjunction with coupled cluster theory to estimate the exchange parameters. We assess this broken-symmetry CC technique in a variety of magnetically coupled small molecules and bridged transition metal dimers.

## II. THEORY

### A. Extracting exchange couplings

Where used, the Heisenberg model is intended to describe the low-energy spin excitations of the system, but such a description is necessarily approximate. Thus the value of the exchange coupling depends in part on the way in which it is extracted from data. Experimentally, values reported in laboratory studies are generally obtained by fitting the measured magnetic susceptibility to predictions based on the Heisenberg model.

Within theoretical approaches, we can easily illustrate the ambiguity in a system with only two spin centers like the ones studied in this work, in which a single value of  $J$  defines the Heisenberg model completely. For example, Fig. 1 shows the spin ladder for  $\text{Fe}_2\text{OCl}_6^{2-}$  computed from spin-averaged complete-active-space self-consistent field (CASSCF) (10,10) orbitals<sup>17</sup> so as to treat all spin states on equal footing and corrected by  $n$ -electron valence second-order perturbation theory (NEVPT2)<sup>18-21</sup> to partially recover the lost correlation from limiting the active space. Choosing the two highest spin states (HS, HS-1) as is done in the procedure of Mayhall and Head-Gordon gives a value of  $J$  that is  $71 \text{ cm}^{-1}$  smaller in magnitude than if the states of lowest multiplicity are used, a discrepancy which is comparable to the  $J$  values

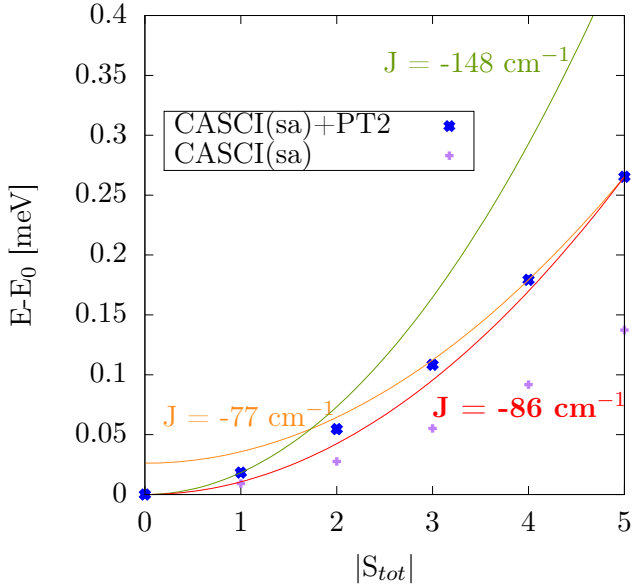


FIG. 1. Theoretical spectrum of  $\text{Fe}_2\text{OCl}_6^{2-}$  as obtained by CASSCF(10,10) and NEVPT2 with orbitals obtained via a spin-average over all spin-states. A simple Heisenberg model cannot exactly capture this spectrum and fits of the Heisenberg model yield exchange couplings that vary by up to a factor of 2 depending on the chosen weighting of the states in the fit. Note that for single-reference methods  $|S_{tot}|$  can differ significantly from integer values.

themselves. A least-squares fit to all states yields  $-85 \text{ cm}^{-1}$ , which is within 10% of the former value, and even closer to that obtained when the lowest spin and highest spin (LS and HS, respectively) states are selected. Note that strong  $S$  dependence of  $J$  in these fits does not necessarily mean that the Heisenberg model is a poor approximation for the molecule itself, because the quality of the theoretical approximations themselves depends on the spin state. Thus we see that, when giving a theoretical value for  $J$  it is important to specify which states were used to compute it, which we do in our work below.

Finally, we stress that it is not necessary, nor always desirable, to fit the exchange parameters of the Heisenberg model to theoretical calculations of spin eigenstates. The basis of an effective model is that there exists a space of low-energy states where the matrix elements of the model Hamiltonian and the *ab initio* Hamiltonian agree, but one is free to choose any rotation within this space to characterize the model parameters. While fitting to eigenstates is convenient, it is undesirable if the theoretical approach incurs a large error for such states. This is the rationale behind broken symmetry approaches, which we now discuss.

## B. Broken symmetry approach to J couplings

One of the earliest proposals to estimate exchange couplings from broken-symmetry wavefunctions was given by Noodleman.<sup>5</sup> His popular method computes magnetic exchange coupling constants using broken symmetry unrestricted Hartree-Fock (BS-UHF) solutions for low-spin states

$$J = \frac{-[E(\text{HS}) - E(\text{BS})]}{s_{max}^2}, \quad (2, \text{"Noodleman"})$$

where  $E(\text{BS})$  is the energy of the low-spin solution,  $E(\text{HS})$  is the high-spin energy, and  $s_{max}$  is the total spin of the high-spin state. This assumes that the broken symmetry state is an equal mixture of the lowest and highest spin states, which is strictly valid only for broken symmetry determinants with two  $s = 1/2$  centers in the weak overlap limit.

A more general approach was suggested by Yamaguchi, originally for DFT calculations.<sup>6</sup> That approach, and its correspondence to that of Noodleman (which is also today applied with DFT calculations),<sup>5</sup> can be developed as follows. Consider two coupled spins  $\mathbf{S}_A$  and  $\mathbf{S}_B$ , for which the resultant spin is

$$\mathbf{S}_{tot}^2 = \mathbf{S}_A^2 + \mathbf{S}_B^2 + 2\mathbf{S}_A \cdot \mathbf{S}_B. \quad (3)$$

Using the definition of  $J_{AB}$ , Eq. 1, the energy of a given state  $\psi$  (not necessarily an eigenstate) is

$$E(\psi) = -J_{AB} [\langle \mathbf{S}_{tot}^2 \rangle - \langle \mathbf{S}_A^2 \rangle - \langle \mathbf{S}_B^2 \rangle], \quad (4)$$

which can be used to determine  $J_{AB}$  by using energies of any two states  $\psi_1$  and  $\psi_2$ , *viz.*

$$J_{AB} = \frac{E(\psi_1) - E(\psi_2)}{\langle \mathbf{S}^2 \rangle_{\psi_2} - \langle \mathbf{S}^2 \rangle_{\psi_1}}. \quad (5)$$

Typically, one chooses  $\psi_1$  to be an approximation to the HS state, which is usually close to a spin eigenfunction with most methods. For the case under consideration then, one can obtain the specific form of the Yamaguchi formula by inserting the HS (T) and BS (S) energies and spins

$$J_{AB} = \frac{E(\psi_T) - E(\psi_S)}{\langle \mathbf{S}^2 \rangle_{\psi_S} - \langle \mathbf{S}^2 \rangle_{\psi_T}}. \quad (8, \text{"Yamaguchi"})$$

For two uncoupled spins, the broken-symmetry UHF singlet solution is roughly “half-singlet” and “half-triplet”, so that  $\langle \mathbf{S}^2 \rangle_{BS} \sim 1$ , the equality of which recovers the Noodleman formula with  $s_{max} = 1$  provided the high-spin wavefunction is a spin eigenfunction. Similarly, for the desired broken symmetry solution in which all unpaired  $\alpha$  spins are on one center, and all unpaired  $\beta$  on the other, it can be shown that  $\langle \mathbf{S}^2 \rangle_{BS} = s_{max}$ , so that the denominator of the Yamaguchi formula reduces to

$$s_{max} - s_{max}(s_{max} + 1) = -s_{max}^2, \quad (7)$$

which serves to show the correspondence between the Yamaguchi and Noodleman equations.

The advantage of the Yamaguchi formula is that it can be applied to any wavefunction for the low-spin state, approximate or exact, while the Noodleman formula (at least in the sense of the correspondence illustrated above) applies only when the broken-symmetry wavefunction is used in its unadulterated form, *i.e.* at the SCF (or Kohn-Sham DFT) level of theory. The accuracy of the Yamaguchi formula then depends on how completely the low-spin state is contained in the linear-span of spin eigenstates that form the model space of the Heisenberg model, and how well the theoretical method captures the expectation value of the energy in such a state. It has been recognized that coupled-cluster (CC) calculations based on broken-symmetry reference functions are an expedient way to obtain reasonably accurate energies in many situations qualitatively described by low-spin electronic configurations,<sup>22</sup> such as in homolytic bond-breaking and some transition states (similar strategies are followed in broken-symmetry DFT, which is often referred to as broken-symmetry unrestricted Kohn-Sham theory (BUKS)). As the expectation value of  $\mathbf{S}^2$  is easily calculated for coupled-cluster wavefunctions,<sup>23</sup> it is thus worthwhile to explore the Yamaguchi formula to calculate magnetic exchange coupling constants using broken-symmetry CC wavefunctions, and such calculations form the core of the work reported here.

### III. ILLUSTRATIVE CALCULATIONS

$J$  values for a series of molecules with bridged spin centers will now be presented, comparing the BS-CC approach described above to the EOM-CC approach described previously by Mayhall and Head-Gordon. For reference, we will also give results obtained by the most commonly used approach, evaluating the Noodleman formula with DFT orbitals, and a few other methods.

#### A. Computational Details

All calculations were carried out in the cc-pVDZ basis<sup>24,25</sup> unless specified otherwise, or in plane-wave bases where denoted by PW. PBE, HF, CAS, EOM, and CCSD(T) results were generated with `pyscf`<sup>17,21,26,27</sup>. Coupled cluster results beyond CCSD(T) were generated with `CFOUR`<sup>28</sup> and the MRCC program of Kállay.<sup>29,30</sup> PW-DFT results were generated in `VASP`<sup>31,32</sup> for a simple check of the robustness of the procedures to computational basis.

For the Gaussian orbital calculations, orbitals were first obtained via a restricted open-shell calculation (ROKS/ROHF) for the HS state. Guess orbitals for the LS solution were derived by localizing the singly occupied space of the ROKS/ROHF solution and assigning  $\alpha$  and  $\beta$  occupancies to them, which were subsequently

converged to the BS-UKS/BS-UHF ground state. In addition, HS UKS orbitals were computed, taking care to break spatial symmetry when present in order to obtain the lowest energy solution.

For the plane-wave calculations projector-augmented-wave (PAW) pseudopotentials<sup>33,34</sup> were employed with a plane-wave cutoff energy of 500 eV and an energy threshold for self-consistency of  $10^{-6}$  eV.

Correlated wavefunction calculations were carried out starting from the Gaussian orbital mean-field solutions. UCCSD calculations were based on the corresponding (HS/LS) HF solution keeping all core orbitals frozen. For the BS approach, the BS-UHF orbitals were used. For the EOM approach, ROHF orbitals were used since this allowed for easier convergence of the EOM amplitudes. To initialize the EOM eigenvectors into the correct space, a small EOM calculation was carried out freezing all but the singly occupied orbitals. The singles amplitudes from this calculation were then taken as an initial guess for the eigenvectors in the full space EOM calculation. Preliminary testing showed  $\mathbf{S}^2$  values computed by CCSD and CCSD(T) to be similar. To avoid large memory requirements for the larger systems,  $\mathbf{S}^2$  values computed by CCSD were used for CCSD(T) as well.

CASCI calculations were performed using ROHF/ROKS orbitals, choosing all singly occupied orbitals as the active space. Further CASCI calculations were performed using orbitals determined from spin-averaged CASSCF calculations over the same space, weighting the HS and LS state equally (CASCI(sa)). Second-order perturbative corrections were calculated for all cases separately via NEVPT2 (denoted “+PT2” below). Because both CASCI and NEVPT2 used a spin-adapted implementation, the spins appearing in the Yamaguchi formula for these methods are equivalent to the spins of the eigenstates.

#### B. Comparison to the full configuration interaction limit

We first look at two cases which can be solved effectively exactly (*i.e.* full CI quality results are available) in Table I. Both model systems comprise two spin- $\frac{1}{2}$  centers coupled via super-exchange into a singlet and a triplet. Both structures are centrosymmetric molecules comprising two hydrogen atoms bridged by a central closed shell atom (X=He, R(H-He)=1.5Å, and F<sup>-</sup>, R(H-F)=2Å).

Applying the Yamaguchi formula, the series of CC methods converges smoothly to the FCI limit. CCSDTQ is exact for H–He–H and CCSDTQPH can already be seen as almost converged for  $[\text{H–F–H}]^-$ , where FCI requires octuple excitations. In routine chemical practice, however, calculations beyond CCSD(T) are rarely feasible. It is encouraging that  $J$  values obtained with BS-CCSD and EOM-CCSD are comparable in both cases and in good agreement with the exact limit. Specifically, they are considerably closer than the traditionally used Noodleman approaches with mean-field methods.

	Noodleman Yamaguchi		$\mathbf{S}_{\text{LS}}^2$
<u>H–He–H</u>			
CCSDTQ	-1126	<b>-563</b>	0.0000
CCSDT	-1120	-560	0.0001
CCSD(T)	-875	-534	—
CCSD	-761	-464	0.6873
HF (ROHF/BS-UHF)	-536	-530	} 0.9883
HF (UHF/BS-UHF)	-450	-444	
PBE (ROKS/BS-UKS)	-1092	-1035	} 0.9450
PBE (UKS/BS-UKS)	-1036	-981	
<u>[H–F–H]<sup>-</sup></u>			
CCSDTQPH	-2550	<b>-1275</b>	0.0000
CCSDTQP	-2548	-1274	0.0000
CCSDTQ	-2520	-1260	0.0004
CCSDT	-2288	-1164	0.0361
CCSD(T)	-1577	-1202	—
CCSD	-1246	-950	0.6880
HF (ROHF/BS-UHF)	-803	-789	} 0.9823
HF (UHF/BS-UHF)	+99	+97	
PBE (ROKS/BS-UKS)	-3748	-2702	} 0.6130
PBE (UKS/BS-UKS)	-3474	-2500	

	H–He–H	[H–F–H] <sup>-</sup>
EOM-CCSD	-554	-1178
PW-LDA	-1435	-2048
PW-PBE	-978	-1589
PW-B3LYP	-1240	-1971
PW-SCAN	-1009	-1450
CASCI(PBE)	-399	+5523
CASCI(PBE)+PT2	-537	-5377
CASCI(HF)	-421	-126
CASCI(HF)+PT2	-519	-940
CASCI(sa)	-508	-425
CASCI(sa)+PT2	-536	-906

TABLE I.  $J$  coupling constants in  $\text{cm}^{-1}$  for H–He–H and [H–F–H]<sup>-</sup> across different methods. FCI quality results are highlighted in bold. For mean-field methods the HS and LS method are given respectively in parenthesis. Since  $\mathbf{S}^2$  are not computed in VASP, the Noodleman formula is used for all PW results. In all PW calculations the HS state is described by UKS.

As the coupled cluster series approaches the exact limit, the corresponding  $\langle \mathbf{S}^2 \rangle_{\text{LS}}$  values have to decay from the broken-symmetry value of the reference determinant to the spin eigenfunction value of zero. Therefore, applying the Noodleman formula with coupled cluster energies with increasing excitation level must converge to the wrong result since it does not take this effect into account. Since the deviation of the spin of the LS state from the broken-symmetry value is already substantial within the CCSD description, especially for H–He–H ( $\mathbf{S}^2 = 0.362$ ), it is critical for the BS-CCSD approach to employ the Yamaguchi and not the Noodleman formula to correct for the non-zero  $\mathbf{S}^2$  value. Without any correction, one would obtain only  $J = -437 \text{ cm}^{-1}$  even with CCSD(T), while

the Noodleman formula would drastically overshoot (see Table I). This difference between the Noodleman and Yamaguchi equations does not occur within the mean-field description for which the Noodleman approach was originally intended, as the BS  $\mathbf{S}^2$  value (0.998) is quite close to the ideal value of 1. We will study in Section III C how important this difference is in real molecular systems. Surprisingly, for the H–He–H case, EOM-CCSD even outperforms BS-CCSD(T). We will see in Section III C that this is not always the case in realistic molecules.

While Noodleman and Davidson originally suggested their equation for HF, it is often used with density functionals instead. While the Noodleman ROHF/BS-UHF results for these cases are only off by up to 37%, the corresponding PBE results can be off by more than a factor of two. Similar results are seen in both the Gaussian and PW basis.

CASCI underestimates the magnitude of the coupling constant since the active space only correlates the valence electrons of the two spin-centers and thus does not capture the super-exchange mechanism. NEVPT2 treats the effect of all other electrons perturbatively and recovers part of the missing correlation. We find that NEVPT2 still underestimates the missing correlation and therefore the magnitude of  $J$ , although it outperforms all mean-field methods independent of whether the Noodleman or Yamaguchi formula are used.

### C. Application to bridged transition metal dimers

We next consider how these findings generalize to realistic bridged transition metal dimers with varying numbers of d-electrons (Figure 2).

The different CC approaches are contrasted in Table II. In line with Mayhall and Head-Gordon<sup>16</sup>, for EOM-CCSD the  $\mathbf{S}^2$  values were not calculated but their idealized values (assuming spin eigenstates for HS and HS-1) were used. All three methods—EOM-CCSD, BS-CCSD, and BS-CCSD(T)—yield comparable results. As in the cases of H–He–H and [H–F–H]<sup>-</sup>, for all systems other than  $\text{Mn}_2\text{O}(\text{CN})_{10}^{6-}$  going from BS-CCSD to BS-CCSD(T) increases the magnitude of  $J$ . In all these cases then, the FCI limit is probably slightly larger in magnitude than the BS-CCSD(T) result. Given this assumption, BS-CCSD(T) performs best across all molecules. There is no clear trend as to whether BS-CCSD or EOM-CCSD performs better.

All three methods are consistent even away from equilibrium geometry. Figure 3 shows the energy curves for  $\text{Ti}_2\text{OCl}_4$  with respect to symmetric stretching of the Ti–O bond distance maintaining all other angles and distances and the corresponding  $J$  values. All methods agree regarding the equilibrium distance and show  $J$  to (properly) decay towards zero as the bond is dissociated at similar rates.

We contrast BS-CCSD(T) and EOM-CCSD with results from mean field calculations as well as

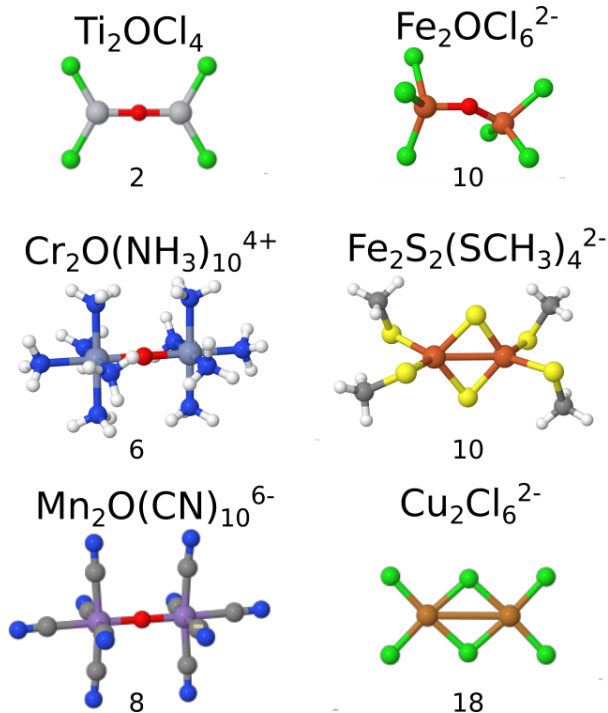


FIG. 2. Bridged transition metal dimers for which  $J$  values are evaluated in Section III C. The total number of  $d$ -electrons is given below each molecule.

CASCI(sa)+PT2 and experiment in Table III. Both CC approaches are broadly consistent with experimental results in all cases. From this, one can surmise that CC methods provide reliable results which can be used to compare with other methods.

While a rigorous benchmark of different mean-field approaches is beyond the scope of this study, the following deserves mention: Hart *et al.*<sup>35</sup> had concluded from studying H-He-H, [H-F-H]<sup>-</sup>, and Ti<sub>2</sub>OCl<sub>4</sub> that the Noodleman formula with HF was performing better when using restricted open-shell rather than unrestricted HS energies. While we can reproduce this effect for the same molecules (in fact, for two of them using unrestricted HS orbitals even yields the wrong sign), this seems not to be true in general. In all cases involving transition-metal systems, the mixed ROHF-UHF approach tends to vastly overestimate the magnitude of the coupling constant.

HF results are off drastically in many cases, regardless of the orbitals and formula chosen (Noodleman or Yamaguchi), even as much as an order of magnitude in the case of Mn<sub>2</sub>O(CN)<sub>10</sub><sup>6-</sup>. The same can be said for PBE results. That the BS-CCSD(T) result is obtained from the same BS-UHF orbitals as the UHF  $J$  values indicates that the rather poor results for the other methods reflect true shortcomings of those methods in the context of these applications. This is even true for CASCI(sa)+PT2 which, apart from this case, follows the same behavior as discussed previously.

	$E(\text{HS})$ ( $S_{\text{HS}}^2$ )	$E(\text{low})$ ( $S_{\text{low}}^2$ )	$J$
	a.u.	a.u.	cm <sup>-1</sup>
<b>Ti<sub>2</sub>OCl<sub>4</sub></b>	-3611...		
EOM-CCSD	.533061	.533283	-24
BS-CCSD	.533126 (2.002079)	.533267 (0.999454)	-31
BS-CCSD(T)	.583558	.583748	-42
<b>Cr<sub>2</sub>O(NH<sub>3</sub>)<sub>10</sub><sup>4+</sup></b>	-2725...		
EOM-CCSD	.426271	.430946	-171
BS-CCSD	.426729 (12.008289)	.433326 (2.910380)	-159
BS-CCSD(T)	.514911	.522934	-194
<b>Mn<sub>2</sub>O(CN)<sub>10</sub><sup>6-</sup></b>	-3300...		
BS-CCSD	.159211 (20.040980)	.189390 (3.805756)	-408
BS-CCSD(T)	.363566	.375919	-167
<b>Fe<sub>2</sub>OCl<sub>6</sub><sup>2-</sup></b>	-5359...		
EOM-CCSD	.119664	.125261	-123
BS-CCSD	.120087 (30.003902)	.131194 (4.796592)	-97
BS-CCSD(T)	.178681	.192750	-123
<b>Fe<sub>2</sub>S<sub>2</sub>(SCH<sub>3</sub>)<sub>4</sub><sup>2-</sup></b>	-5071...		
BS-CCSD	.020339 (30.014220)	.038130 (4.699074)	-154
BS-CCSD(T)	.107047	.129098	-191
<b>Cu<sub>2</sub>Cl<sub>6</sub><sup>2-</sup></b>	-6037...		
EOM-CCSD	.368900	.368900	-0
BS-CCSD	.369189 (2.001204)	.369169 (0.998728)	4
BS-CCSD(T)	.414833	.414886	-12

TABLE II. State-specific absolute energies and  $J$  values computed via EOM-CCSD, BS-CCSD, and BS-CCSD(T). For EOM “low” denotes the HS-1 state, for BS the broken-symmetry LS state. The EOM HS energy is obtained from ROHF orbitals, the BS HS energies from UHF orbitals. The exact values for  $S_{\text{HS}}^2$  and  $S_{\text{HS-1}}^2$  were used for the evaluation of  $J$  from EOM to reproduce the procedure used by Mayhall and Head-Gordon.<sup>16</sup> For BS-CCSD(T) the  $S^2$  values computed with BS-CCSD were used.

One interesting finding in this study concerns the values of  $\langle S^2 \rangle$  for the BS-CC wavefunctions. While the small systems that are treated in Section III B are such that correlation at the CCSD level acts to significantly reduce the LS  $\langle S^2 \rangle$  value from the near-unity value of the reference determinant, it turns out that this is not true for the transition metals, where the correlation contribution to  $\langle S^2 \rangle$  is rather small. It seems that in these cases, the electrons within the spin-centers are being more “correlated” than are the interactions between electrons on different spin centers. Because of this, it is apparent that the simple Noodleman equation – which does not require the (somewhat expensive) calculation of  $\langle S^2 \rangle$  can be applied in conjunction with the BS-CC wavefunctions. We verify this in Table IV and find that indeed this approach yields results almost identical to full BS-CCSD and BS-CCSD(T) respectively. It is important to note that this simpler approach appears to work well in practice (with less than triples excitations). As discussed previously,

Spin Descr. J [cm <sup>-1</sup> ]	Yamaguchi CCSD(T)	Mayhall EOM-CCSD	Noodleman ROHF	Noodleman UHF	Yamaguchi UKS (PBE)	Yamaguchi CASCI(sa)+PT2	Experiment
Ti <sub>2</sub> OCl <sub>4</sub>	-41	-24	-982	+3	-77	-12	— <sup>a</sup>
Cr <sub>2</sub> O(NH <sub>3</sub> ) <sub>10</sub> <sup>4+</sup>	-194 <sup>b</sup>	-171	-424	-60	-356	-89	-225 <sup>c</sup>
Mn <sub>2</sub> O(CN) <sub>10</sub> <sup>6-</sup>	-167 <sup>b</sup>	— <sup>d</sup>	-2966	-1238	-2085	-2000	-360 <sup>e</sup>
Fe <sub>2</sub> OCl <sub>6</sub> <sup>2-</sup>	-123	-123	-164	-23	-246	-70	-112 <sup>f</sup>
Fe <sub>2</sub> S <sub>2</sub> (SCH <sub>3</sub> ) <sub>4</sub> <sup>2-</sup>	-191 <sup>b</sup>	— <sup>g</sup>	-433	-54	-850	-111	-148 <sup>h</sup>
Cu <sub>2</sub> Cl <sub>6</sub> <sup>2-</sup>	-12	0	-1720	+24	-140	-4	-19 <sup>i</sup>

<sup>a</sup> no experimental result available. Geometry taken from Hart *et al.*<sup>35</sup> at R(Ti-O)=1.8 Å.

<sup>b</sup>  $\mathbf{S}^2$  values computed from analogous calculation with def-sv basis on the outer ligands due to memory limitations (energies full cc-pvdz)

<sup>c</sup> from Pedersen<sup>36</sup>. Geometry taken from Harris *et al.*<sup>37</sup> who reported J=-124 cm<sup>-1</sup>.

<sup>d</sup> UCCSD did not converge due to the large ROHF→UHF instability of the HS state ( $\Delta E=3.3$  eV,  $\Delta \mathbf{S}^2=0.74$ ).

<sup>e</sup> estimated from Ziolo *et al.*<sup>38</sup> by fitting the measured magnetic moment to a two-site Heisenberg model. The experimental result may be smaller due to unknown amounts of paramagnetic impurities in the sample.

<sup>f</sup> from Haselhorst *et al.*<sup>39</sup>. Geometry taken from Harris *et al.*<sup>37</sup> who reported J=-117 cm<sup>-1</sup>.

<sup>g</sup> UCCSD did not converge due to large ROHF→UHF instability of the HS state ( $\Delta E=1.9$  eV,  $\Delta \mathbf{S}^2=0.06$ ).

<sup>h</sup> from Gillum *et al.*<sup>40</sup> for the synthetic analog Fe<sub>2</sub>S<sub>2</sub>(S<sub>2</sub>-o-oxyl)<sub>2</sub><sup>2-</sup>. Geometry taken from Sharma *et al.*<sup>41</sup> who report J=-236 cm<sup>-1</sup>.

<sup>i</sup> from Maass, Gerstein, and Willett<sup>42</sup>. Geometry taken from Willett *et al.*<sup>43</sup>.

TABLE III. Comparison of  $J$  values computed by broken-symmetry CCSD(T) to those obtained with EOM-CCSD for a series of molecules depicted in Figure 2. HF and PBE results from UHF and UKS calculations as well as CASCI(sa)+PT2, and experimental results are given for reference. Results obtained from the commonly used Noodleman approximation with ROHF and BS-UHF energies as suggested by Hart *et al.*<sup>35</sup> are also given. In the procedure described in Section III A for the evaluation of EOM-CCSD, a large ROHF→UHF instability leads to convergence problems for the CCSD calculation underlying EOM-CCSD in two cases (Mn<sub>2</sub>O(CN)<sub>10</sub><sup>6-</sup>:  $\Delta E=3.3$  eV,  $\Delta \mathbf{S}^2=0.74$ ; Fe<sub>2</sub>S<sub>2</sub>(SCH<sub>3</sub>)<sub>4</sub><sup>2-</sup>:  $\Delta E=1.9$  eV,  $\Delta \mathbf{S}^2=0.06$ ). In all other cases  $\Delta E$  is 0.4 eV or less and  $\Delta \mathbf{S}^2$  at most 0.03. ( $\Delta E$  and  $\Delta \mathbf{S}^2$  represent the change in energy and squared spin between ROHF and UHF).

	Noodleman		Yamaguchi		EOM CCSD
	CCSD(T)	CCSD	CCSD(T)	CCSD	
Ti <sub>2</sub> OCl <sub>4</sub>	-42	-31	-42	-31	-24
Cr <sub>2</sub> O(NH <sub>3</sub> ) <sub>10</sub> <sup>4+</sup>	-196	-161	-194	-159	-171
Mn <sub>2</sub> O(CN) <sub>10</sub> <sup>6-</sup>	-169	-414	-167	-408	
Fe <sub>2</sub> OCl <sub>6</sub> <sup>2-</sup>	-124	-98	-123	-97	-123
Fe <sub>2</sub> S <sub>2</sub> (SCH <sub>3</sub> ) <sub>4</sub> <sup>2-</sup>	-194	-156	-191	-154	
Cu <sub>2</sub> Cl <sub>6</sub> <sup>2-</sup>	-12	4	-12	4	0

TABLE IV. Comparison of  $J$  coupling constants computed from CCSD and CCSD(T) energies and consistently evaluated  $\mathbf{S}^2$  values (Yamaguchi) and with theoretical HS/BS  $\mathbf{S}^2$  values in comparison (Noodleman). EOM-CCSD values are given for reference.

however, it is apparent that as one converges the level of CC excitations in these molecules,  $\langle \mathbf{S}^2 \rangle$  will tend to zero and this approach has to eventually converge to the wrong limit. We have seen this in Section III B, where due to the small size of the molecules already CCSD resulted in significantly reduced  $\langle \mathbf{S}^2 \rangle$  values.

#### IV. CONCLUSION

This work demonstrates that a simple application of the broken-symmetry approach for calculating magnetic exchange coupling constants in conjunction with coupled-cluster theory provides useful results in practice. As such, this method complements recent work by Mayhall and Head-Gordon that has used the spin-flip variant

of equation-of-motion coupled cluster theory. The two approaches both rely on fitting  $J$  to two energies; the present method uses the highest and broken-symmetry lowest-spin state, while the EOM-CC method uses the two highest spin states. Note that there is no formal disadvantage to using broken symmetry states so long as the  $\langle \mathbf{S}^2 \rangle$  values are computed for the states of interest, as in the formula of Yamaguchi. However, we have also shown that the simpler approach of Noodleman, which posits the value of  $\langle \mathbf{S}^2 \rangle$  for the broken-symmetry lowest-spin state, works as well in practice for many realistic molecules.

Computations by the present method are quite straightforward; one needs only to find BS solutions to the self-consistent field equations to obtain a reference single determinant, and to evaluate coupled-cluster energies and (optionally) one- and two-electron density matrix elements ( $\langle \mathbf{S}^2 \rangle$  is straightforwardly computed from these) if the Yamaguchi formula is used. In particular, one does not need to wrestle with converging the EOM-CC equations or assigning spin states, which is not always straightforward.<sup>16</sup> In our experience, iterative solvers to the EOM equations can get stuck on higher energy solutions unless initial guesses are constructed very carefully. While we studied binary systems with only a single  $J$  coupling in this work, in many cases one is interested in finding  $J$  for each of multiple interactions in a molecule separately. BS coupled cluster methods can then potentially be applied the same way as BS DFT – by spin flipping into separate configurations.

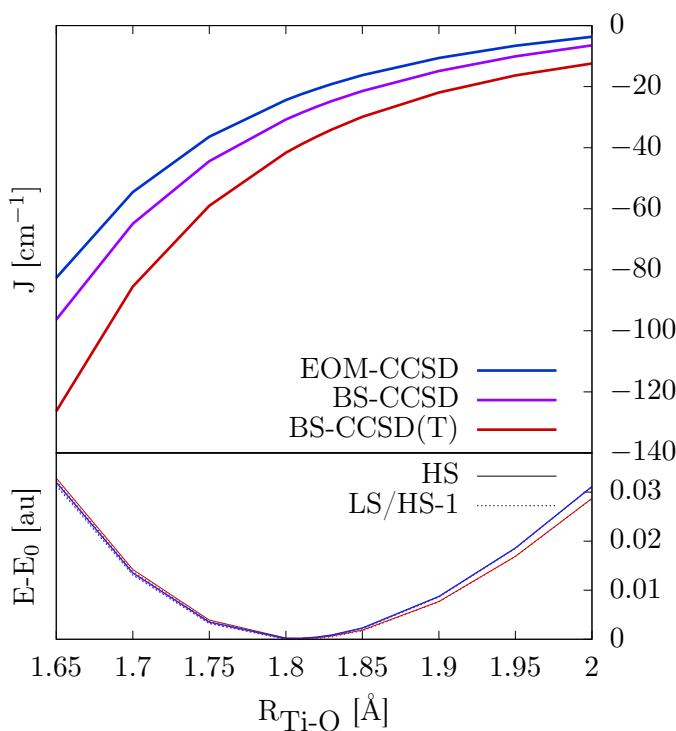


FIG. 3.  $J$  coupling constants (top) and HS and LS energies (bottom) with BS-CCSD, BS-CCSD(T) and EOM-CCSD (HS-1 instead of LS for the EOM calculation). Note that in the lower panel, the LS curves are almost directly under the HS curves due to the small size of the exchange coupling on this scale. For each of the three methods the energy curves have been shifted by their respective LS equilibrium energies,  $E_0$ . All three methods qualitatively agree near equilibrium, with BS-CCSD(T) starting to visually differ at stretched distances. Nonetheless, the resulting  $J$  coupling constant distance dependence is similar in all methods even when the absolute energies start to differ.

Calibrating other methods may be one of the main uses of more accurate methods to determine exchange couplings. Since both the EOM and BS coupled cluster approaches agree broadly with experiment and yield consistent results across all studied systems even away from equilibrium, they represent a reliable gauge by which to assess the accuracy of other methods. This is especially valuable since we observe very different behavior for different classes of molecules. For example, we can confirm that in small model systems using the commonly applied Noodleman formula with ROHF energies instead of UHF energies for the HS state yields superior results as posited by Hart *et al.*<sup>35</sup> However, we observe the same not to be true for the larger transition metal complexes.

In short, broken-symmetry coupled cluster theory provides a straightforward methodology to predict magnetic exchange coupling constants, complementing approaches that target spin-eigenstates, such as equation-of-motion coupled cluster methods and complete-active-space tech-

niques. It is especially reliable when employing the Yamaguchi equation, in which case it can cope with almost arbitrary amounts of spin contamination.

## V. ACKNOWLEDGEMENTS

This work was supported as part of the Center for Molecular Magnetic Quantum Materials, an Energy Frontier Research Center funded by the U.S. Department of Energy, Office of Science, Basic Energy Sciences under Award No. de-sc0019330. Computations were performed at NERSC, UFRC, and on the Caltech HPC cluster. HFS acknowledges funding from the European Union’s Framework Programme for Research and Innovation Horizon 2020 (2014-2020) under the Marie Skłodowska-Curie Grant Agreement No. 754388 and from LMUexcellent as part of LMU Munich’s funding as a University of Excellence within the framework of the German Excellence Strategy.

<sup>1</sup>P. A. M. Dirac, Proc. R. Soc. A **112**, 661 (1926).

<sup>2</sup>W. Heisenberg, Zeitschrift für Phys. **49**, 619 (1928).

<sup>3</sup>J. H. van Vleck, *The Theory of Electric and Magnetic Susceptibilities* (Clarendon Press, Oxford, 1932).

<sup>4</sup>P. W. Anderson, Phys. Rev. **115**, 2 (1959).

<sup>5</sup>L. Noodleman, J. Chem. Phys. **74**, 5737 (1981).

<sup>6</sup>K. Yamaguchi, Y. Takahara, and T. Fueno, in *Appl. Quantum Chem.*, edited by V. H. Smith, H. F. Schaefer, and K. Morokuma (Springer Netherlands, Dordrecht, 1986) pp. 155–184.

<sup>7</sup>L. Noodleman and E. R. Davidson, Chem. Phys. **109**, 131 (1986).

<sup>8</sup>M. Nishino, S. Yamanaka, Y. Yoshioka, and K. Yamaguchi, J. Phys. Chem. A **101**, 705 (1997).

<sup>9</sup>R. Caballol, O. Castell, F. Illas, I. de P. R. Moreira, and J. P. Malrieu, J. Phys. Chem. A **101**, 7860 (1997).

<sup>10</sup>E. Ruiz, J. Cano, S. Alvarez, and P. Alemany, J. Comput. Chem. **20**, 1391 (1999).

<sup>11</sup>E. Ruiz, in *Princ. Appl. Density Funct. Theory Inorg. Chem. II* (Springer Berlin Heidelberg, 2004) pp. 71–102.

<sup>12</sup>I. Rudra, Q. Wu, and T. Van Voorhis, J. Chem. Phys. **124**, 024103 (2006).

<sup>13</sup>P. Comba, S. Hausberg, and B. Martin, J. Phys. Chem. A **113**, 6751 (2009).

<sup>14</sup>D. A. Pantazis, V. Krewald, M. Orto, and F. Neese, Dalt. Trans. **39**, 4959 (2010).

<sup>15</sup>I. Shavitt and R. J. Bartlett, *Many Body Methods in Chemistry and Physics* (Cambridge University Press, Cambridge, 2009).

<sup>16</sup>N. J. Mayhall and M. Head-Gordon, J. Chem. Phys. **141**, 134111 (2014).

<sup>17</sup>Q. Sun, J. Yang, and G. K. L. Chan, Chem. Phys. Lett. **683**, 291 (2017).

<sup>18</sup>C. Angeli, R. Cimiraglia, S. Evangelisti, T. Leininger, and J.-P. Malrieu, J. Chem. Phys. **114**, 10252 (2001).

<sup>19</sup>C. Angeli, R. Cimiraglia, and J.-P. Malrieu, Chem. Phys. Lett. **350**, 297 (2001).

<sup>20</sup>C. Angeli, R. Cimiraglia, and J.-P. Malrieu, J. Chem. Phys. **117**, 9138 (2002).

<sup>21</sup>S. Guo, M. A. Watson, W. Hu, Q. Sun, and G. K.-L. Chan, J. Chem. Theory Comput. **12**, 1583 (2016).

<sup>22</sup>T. Saito, N. Yasuda, Y. Kataoka, Y. Nakanishi, Y. Kitagawa, T. Kawakami, S. Yamanaka, M. Okumura, and K. Yamaguchi, J. Phys. Chem. A **115**, 5625 (2011).

<sup>23</sup>J. F. Stanton, J. Chem. Phys. **101**, 371 (1994).

<sup>24</sup>T. H. Dunning, Jr., J. Chem. Phys. **90**, 1007 (1989).

<sup>25</sup>D. E. Woon and T. H. Dunning, Jr., J. Chem. Phys. **98**, 1358 (1993).

- <sup>26</sup>Q. Sun, T. C. Berkelbach, N. S. Blunt, G. H. Booth, S. Guo, Z. Li, J. Liu, J. D. McClain, E. R. Sayfutyarova, S. Sharma, S. Wouters, and G. K.-L. Chan, *WIREs Comput. Mol. Sci.* **8**, e1340 (2018).
- <sup>27</sup>PySCF, “<https://github.com/pyscf/pyscf>,” (2019).
- <sup>28</sup>J. Stanton, J. Gauss, L. Cheng, M. Harding, D. Matthews, P. Szalay, A. Auer, R. Bartlett, U. Benedikt, C. Berger, D. Bernhard, Y. Bomble, O. Christiansen, F. Engel, R. Faber, M. Heckert, O. Heun, M. Hilgenberg, C. Huber, T.-C. Jagau, D. Jansson, J. Jusélius, T. Kirsch, K. Klein, W. Lauderdale, F. Lipparini, T. Metzroth, L. Mück, D. O’Neill, D. Price, E. Prochnow, C. Puzzarini, K. Ruud, F. Schiffmann, W. Schwalbach, C. Simmons, S. Stopkowitz, A. Tajti, J. Vázquez, F. Wang, J. Watts, P. Taylor, J. Almlöf, T. Helgaker, H. A. Jensen, P. Jørgensen, J. Olsen, C. van Wüllen., and A. V. Mitin, “CFOUR, Coupled-Cluster techniques for Computational Chemistry, a quantum-chemical program package,” (2019).
- <sup>29</sup>M. Kállay, P. R. Nagy, Z. Rolik, D. Mester, G. Samu, J. Csontos, J. Csóka, B. P. Szabó, L. Gyevi-Nagy, I. Ladjánszki, L. Szegedy, B. Ladóczki, K. Petrov, M. Farkas, P. D. Mezei, and B. Hégyel, “MRCC, a quantum chemical program suite,” (2019).
- <sup>30</sup>Z. Rolik, L. Szegedy, I. Ladjánszki, B. Ladóczki, and M. Kállay, *J. Chem. Phys.* **139**, 094105 (2013).
- <sup>31</sup>G. Kresse and J. Furthmüller, *Comput. Mater. Sci.* **6**, 15 (1996).
- <sup>32</sup>G. Kresse and J. Furthmüller, *Phys. Rev. B - Condens. Matter Mater. Phys.* **54**, 11169 (1996).
- <sup>33</sup>P. E. Blöchl, *Phys. Rev. B* **50**, 17953 (1994).
- <sup>34</sup>G. Kresse and D. Joubert, *Phys. Rev. B* **59**, 1758 (1999).
- <sup>35</sup>J. R. Hart, A. K. Rappe, S. M. Gorun, and T. H. Upton, *J. Phys. Chem.* **96**, 6264 (1992).
- <sup>36</sup>E. Pedersen, *Acta Chem. Scand.* **26**, 333 (1972).
- <sup>37</sup>T. V. Harris, Y. Kurashige, T. Yanai, and K. Morokuma, *J. Chem. Phys.* **140**, 054303 (2014).
- <sup>38</sup>R. F. Ziolo, R. H. Stanford, G. R. Rossman, and H. B. Gray, *J. Am. Chem. Soc.* **96**, 7910 (1974).
- <sup>39</sup>G. Haselhorst, K. Wieghardt, S. Keller, and B. Schrader, *Inorg. Chem.* **32**, 520 (1993).
- <sup>40</sup>W. O. Gillum, R. B. Frankel, S. Foner, and R. H. Holm, *Inorg. Chem.* **15**, 1095 (1976).
- <sup>41</sup>S. Sharma, K. Sivalingam, F. Neese, and G. K.-L. Chan, *Nat. Chem.* **6**, 927 (2014).
- <sup>42</sup>G. J. Maass, B. C. Gerstein, and R. D. Willett, *J. Chem. Phys.* **46**, 401 (1967).
- <sup>43</sup>R. D. Willett, C. Dwiggin, R. F. Kruh, and R. E. Rundle, *J. Chem. Phys.* **38**, 2429 (1963).